Astronomy & Astrophysics

Interstellar H$_2$ toward HD 37903*

P. Gnaciński

Institute of Theoretical Physics and Astrophysics, University of Gdańsk, ul. Wita Stwosza 57, 80-952 Gdańsk, Poland
e-mail: pg@iftia9.univ.gda.pl

ABSTRACT

We present an analysis of interstellar H$_2$ toward HD 37903, which is a hot B 1.5 V star located in the NGC 2023 reflection nebula. Meyer et al. (2001, ApJ, 553, L59) used a rich spectrum of vibrationally excited H$_2$ observed by the HST to calculate a model of the interstellar cloud toward HD 37903. We extend their analysis by including the $v'' = 0$ vibrational level observed by the FUSE satellite. The temperature calculated from the two lowest rotational levels ($J'' = 0, 1$) of the H$_2$ molecule should not be interpreted as a "rotational temperature", but rather as a temperature of thermal equilibrium between the ortho and para H$_2$. The ortho-to-para H$_2$ ratio is lower for the lowest rotational levels than for the higher levels populated by fluorescence. The PDR model of the cloud located in front of HD 37903 points to a gas kinetic temperature ranging from 110 K on the observer side of the cloud to 377 K on the star side. The hydrogen density changes from $n_{\rm H} = 1874$ cm^{-3} on the observer side to 544 cm^{-3} on the star side. The star-cloud distance in our model is 0.45 pc.

Key words. ISM: molecules – photon-dominated region (PDR) – ISM: general

1. Introduction

A rich spectrum of vibrationally excited H$_2$ in the direction to HD 37903 was first described by Meyer et al. (2001). They observed over 500 interstellar H$_2$ absorption lines from excited vibrational levels $v'' = 1-14$ and rotational levels up to $J'' = 13$. These lines were detected in a *Hubble* Space Telescope (HST) spectrum made with the Space Telescope Imaging Spectrograph (STIS). A Far Ultraviolet Spectroscopic Explorer (FUSE) spectrum was made after this publication allowing access to the $v'' = 0$ vibrational level of the ground electronic state. The FUSE spectrum had been used by Rachford et al. (2009) to determine the $T_{\rm OP} = 170$ K/ln($9N_0/N_1$) = 68 ± 7 K gas "kinetic" temperature and the hydrogen molecular fraction f(H$_2$) = $2N$(H$_2$)/($2N$(H$_2$)+N(HI)) = 0.53 ± 0.09 in the direction towards HD 37903.

The star HD 37903 was also observed by the Berkeley Extreme and Far–Ultraviolet Spectrometer (BEFS) onboard the Orbiting and Retrievable Far and Extreme Ultraviolet Spectrometer (ORFEUS) telescope. The spectral resolution was $R = 3000$. Lee et al. (2002) have used this spectra to obtain H$_2$ column densities on $v'' = 0$ and $J'' = 0-5$ rotational levels. Their column densities agree within an order of magnitude to the column densities derived in this paper from the FUSE spectra. The physical parameters derived by Lee et al. (2002) are $T_{\rm OP} = 63 \pm 5$ K, f(H$_2$) = 0.496 ± 0.017, and the cloud density $n = 5600$ cm^{-3}.

The H$_2$ molecule exists in two forms: ortho (odd J'') and para (even J'') H$_2$. It is caused by the spins of the hydrogen nuclei, which can point "in the same" direction (ortho H$_2$ – triplet state, total nuclei spin $I = 1$) or in opposite directions (para H$_2$ – singlet state, $I = 0$). The ratio ortho/para H$_2$ (O/P) is therefore 3:1 at standard temperature and pressure. Conversion between these two spin isomers can take place in gas phase or on the surface of gas grains (Le Bourlot 2000). The ortho-para conversion in the gas phase is caused by the exchange of proton in collisions with H, H$^+$, and H$_3^+$.

The fluorescence cascade of H$_2$ that leads to populating the excited ro-vibrational states of H$_2$, as well as to the emission of infrared photons from quadrupole transitions was described by Black & Dalgarno (1976). The first ultraviolet detection of vibrationally excited interstellar H$_2$ was performed by Federman et al. (1995) in the HST spectrum of ζ Ophiuchi.

Section 2 presents the HST and FUSE spectra used in this paper and describes the procedure of calculating the H$_2$ column densities of ro-vibrational energy levels. Section 3 describes the calculation of H$_2$ rotational temperatures, especially the temperatures calculated across the ortho-para divide. Section 4 presents a PDR model of the cloud toward HD 37903.

2. Column densities

We used both HST STIS and FUSE spectra to obtain column densities on H$_2$ ro-vibrational levels. The HST STIS spectrum o59s04010 was averaged because it consists of two subexposures. The HST spectrum is located between 1160 and 1357 Å. We also used the FUSE observation P1160601. We analyzed only spectra from the detectors LiF 1B and LiF 1A. These two spectra have the highest quality. The FUSE spectra coming from the same detector were shifted and coadded using the IRAF tasks *poffsets* and *specalign*. A part of the FUSE spectrum is shown in Fig. 1. The whole FUSE spectrum ranges from 987 Å to 1188 Å.

The Ar I 1048 Å line that lies in the wing of R(0) and R(1) lines was cut out from the spectrum. The wings of H$_2$ lines were calculated up to 60 Å from the line center. The absorption lines in the FUSE spectrum were modeled with the Voigt function,
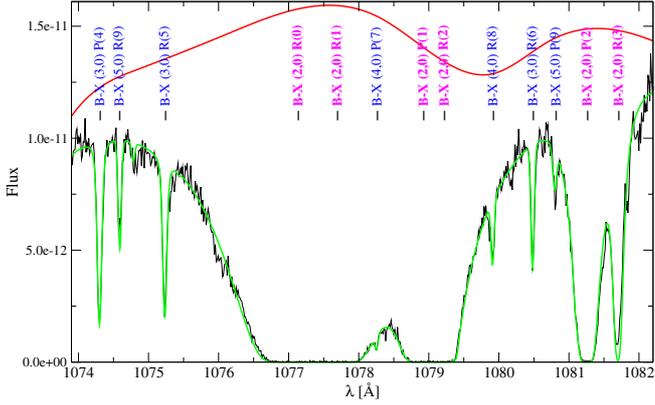
Fig. 1. Fragment of FUSE spectrum with a fit (green line) of H_2 absorption lines. The red line represents continuum.

Fig. 2. Fragment of HST STIS spectrum (gray line with dots) fitted with 268 H_2 absorption lines (green line). The figure presents only a 5 Å fragment of the spectrum, while the presented fit was done to the whole 200 Å long STIS spectrum (1160–1357 Å) and included 7449 H_2 lines.

while a Gauss function was used for modeling the H_2 lines in the STIS spectrum.

We used a Gaussian point spread function (PSF) with *FWHM* equal to 15 km s^{-1} (Jensen et al. 2010) to model the FUSE spectra. The column densities at $J'' = 0$, 1 and 2 ($v'' = 0$) were derived from transitions between B and X electronic levels. The vibrational transitions used are (0, 0), (2, 0), (3, 0), and (4, 0), where the first digit is the v' on the upper electronic level B and the second digit $v'' = 0$ is the vibrational level of the ground electronic state X. The FUSE spectrum at the (1, 0) vibrational transition was too noisy to perform a good fit. The H_2 line positions and oscillator strengths were adopted from Abgrall et al. (1994). The total transition probabilities that include the transitions to continuum (dissociating) states were taken from Abgrall et al. (2000).

The column densities of rotational levels $J'' = 0$–9 from the vibrational $v'' = 0$ level, as well as the column density of the $v'' = 1$ $J'' = 0$ level, were derived from the FUSE spectrum. Other ro-vibrational levels of the X ground electronic state were derived from the o59s04010 HST STIS spectrum. The continuum level for the FUSE spectrum was placed manually in an iterative process of fitting column densities and changing the continuum level.

The column densities were derived with the profile fitting technique. At each point of the simulated spectrum, the optical depth of many spectral lines was summed. Such a procedure is needed to calculate the profile of blended lines which are ubiquitous in the spectra. The cloud velocity, the doppler broadening parameter and column densities on all observed levels were free parameters, which were fitted to the observed spectra. The cloud velocity and the doppler broadening parameter were common for all H_2 absorption lines.

The STIS spectrum was fitted with H_2 absorption lines from all vibrational $v'' = 0$–14 levels, and rotational levels $J'' = 0$–13. H_2 lines that were blended with atomic lines were excluded from the fitting procedure. Total 7449 H_2 lines were included in the simulated STIS spectrum. The whole STIS spectrum (200 Å long) was fitted at once with all 7449 H_2 lines, because of the large number of blended lines. A fragment of the HST STIS spectrum with lines of vibrationally excited molecular hydrogen is presented in Fig. 2. The observed column densities are presented in Table 1 and in Fig. 3. The errors of the column density are about 20% for $J'' = 0$–7 rotational levels, and up to ~40% for higher rotational levels.
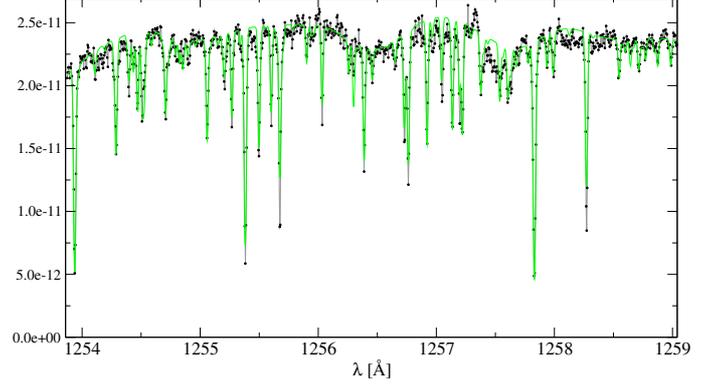
3. Results

The total observed column density of H_2 on all vibrational and rotational levels equals $N(H_2) = (9.6 \pm 1.6) \times 10^{20}$ cm^{-2}. The observed H_2 column density is slightly higher than $N(H_2) = 4 \times 10^{20}$ cm^{-2}, as estimated by Meyer et al. (2001). The column density of neutral hydrogen is $N(HI) = 1.48 \times 10^{21}$ cm^{-2} (Diplas & Savage 1994). The hydrogen molecular fraction (assuming 10% error of $N(HI)$) equals $f(H_2) = 2N(H_2)/(2N(H_2) + N(HI)) = 0.56 \pm 0.04$.

The T_{OP} temperature, calculated from the lowest energy levels of ortho and para H_2 ($v'' = 0$), was derived from the equation:

$$\frac{N(1)}{N(0)} = \frac{g_I(1)g_J(1)}{g_I(0)g_J(0)} \exp\left(-\frac{E(1) - E(0)}{kT_{OP}}\right), \tag{1}$$

where g_I is the spin degeneracy factor $g_I(I) = 2I + 1$. The $g_I(1) = 3$ is the statistical weight for ortho H_2, and the $g_I(0) = 1$ for the para–H_2 spin izomer. The formula $g_J(J) = 2J + 1$ is the statistical weight for the rotational level J. The T_{OP} is the temperature of thermal equilibrium between the ortho and para spin izomers. The derived $T_{OP} = 67 \pm 8$ K is similar to the temperatures determined by Rachford et al. (2009) (68 K) and by Lee et al. (2002) (63 K). The photon-dominated region (PDR) models of interstellar clouds show that the T_{OP} temperature is correlated to the gas kinetic temperature (Le Petit et al. 2006).

However, if we want to calculate the rotational temperature across the ortho-para divide, we have to take the N_{ortho}/N_{para} H_2 ratio into account. The population of the ro-vibrational levels of H_2 depends not only on the temperature and radiation field, but also on the total ortho to para ratio. To include the O/P in the Boltzmann equation, we write separate Boltzmann distributions for the ortho and para spin izomers. The Boltzmann distribution for the ortho H_2 can be written as

$$N_o(J''_o) = \frac{N_{ortho}}{Z_o(T)} g_I(1)g_J(J''_o) \exp\left(-\frac{E(J''_o)}{kT}\right) \tag{2}$$

where N_{ortho} is the total amount of ortho H_2. The partition function Z is

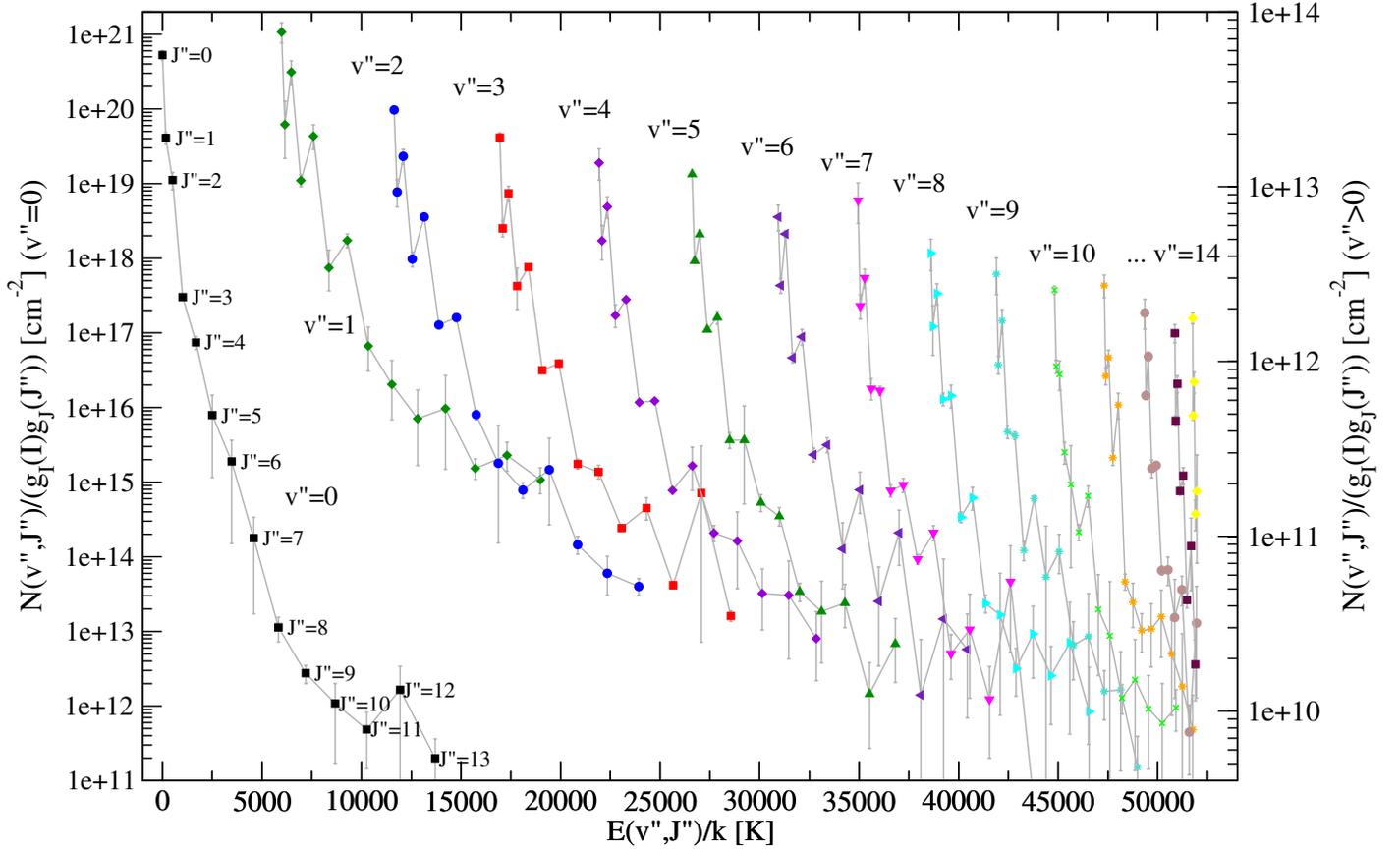$$Z_o(T) = \sum_{J''_o \text{ odd}} g_I(1)g_J(J''_o) \exp\left(-\frac{E(J''_o)}{kT}\right). \tag{3}$$

Fig. 3. Occupation of H$_2$ X ro-vibrational levels towards HD 37903. Note the different y-axis scale for $v'' = 0$ (*left*) and for higher v'' levels (*right*).

Table 1. Column densities of the H$_2$ ro-vibrational levels towards HD 37903 [cm^{-2}].

$J''\backslash v''$	0	1	2	3	4	5	6	7	8	9	10	11	12	13	14
0	5.3e20	7.7e13	2.7e13	1.9e13	1.4e13	1.2e13	6.7e12	8.3e12	4.2e12	3.2e12	2.6e12	2.7e12	1.9e12	1.5e12	1.8e12
1	3.7e20	2.0e14	8.4e13	5.2e13	4.4e13	3.4e13	2.4e13	1.9e13	1.4e13	8.6e12	8.4e12	7.4e12	5.7e12	4.1e12	4.4e12
2	5.6e19	2.3e14	7.4e13	4.6e13	3.8e13	2.7e13	2.7e13	1.5e13	1.2e13	8.6e12	4.2e12	5.3e12	5.3e12	3.7e12	3.8e12
3	6.3e18	2.3e14	8.1e13	5.7e13	3.9e13	3.2e13	2.2e13	1.5e13	1.3e13	8.3e12	6.3e12	5.9e12	5.1e12	3.8e12	2.8e12
4	6.7e17	1.8e14	6.1e13	3.1e13	2.0e13	1.6e13	1.2e13	6.1e12	5.7e12	3.4e12	1.8e12	5.1e12	2.3e12	2.0e12	1.6e12
5	2.6e17	1.1e14	5.3e13	2.9e13	1.9e13	1.2e13	9.7e12	6.0e12	4.2e12	2.7e12	3.5e12	1.8e12	2.1e12	1.4e12	—
6	2.5e16	6.4e13	2.3e13	1.3e13	7.7e12	4.6e12	4.3e12	2.6e12	2.2e12	2.1e12	2.2e12	5.5e11	8.3e11	1.1e12	—
7	8.0e15	5.5e13	2.2e13	1.2e13	8.2e12	7.0e12	3.8e12	3.3e12	1.9e12	2.6e12	1.7e12	1.3e12	1.5e12	8.3e11	—
8	1.9e14	1.3e13	4.4e12	4.0e12	4.3e12	2.2e12	3.1e12	1.8e12	6.0e11	1.4e12	4.6e11	5.0e11	8.4e11	—	—
9	1.6e14	2.7e13	1.0e13	6.4e12	5.9e12	2.7e12	2.4e12	1.2e12	1.0e12	1.4e12	6.8e11	2.0e12	4.3e11	—	—
10	2.3e13	1.1e13	5.0e12	3.0e12	2.0e12	7.8e11	2.2e12	6.2e11	5.8e11	5.6e11	3.2e11	4.5e11	6.7e11	—	—
11	3.3e13	1.7e13	6.2e12	3.6e12	3.2e12	2.9e12	8.5e11	8.1e11	1.1e12	8.9e11	7.1e11	9.5e11	—	—	—
12	4.1e13	7.3e12	1.5e12	4.4e12	1.2e12	3.1e11	8.4e11	1.4e12	6.2e11	3.3e11	2.1e11	2.0e11	—	—	—
13	1.6e13	1.7e13	4.2e12	2.8e12	2.1e12	2.0e12	1.8e12	3.0e11	8.1e11	3.9e11	8.5e11	—	—	—	—

We assume that para H$_2$ has a Boltzmann distribution with the same rotational temperature,

$$N_{\rm p}(J''_{\rm p}) = \frac{N_{\rm para}}{Z_{\rm p}(T)} g_I(0) g_J(J''_{\rm p}) \exp\left(-\frac{E(J''_{\rm p})}{kT}\right), \quad (4)$$

where $N_{\rm para}$ is the total amount of para H$_2$, and the partition function for para H$_2$

$$Z_{\rm p}(T) = \sum_{J''_{\rm p}\ {\rm even}} g_I(0) g_J(J''_{\rm p}) \exp\left(-\frac{E(J''_{\rm p})}{kT}\right). \quad (5)$$

By dividing Eqs. (2) by (4) we obtain

$$\frac{N_{\rm o}(J''_{\rm o})}{N_{\rm p}(J''_{\rm p})} = \frac{N_{\rm ortho}}{N_{\rm para}} \frac{g_I(1) g_J(J''_{\rm o})}{g_I(0) g_J(J''_{\rm p})} \frac{Z_{\rm p}(T)}{Z_{\rm o}(T)} \exp\left(-\frac{E(J''_{\rm o}) - E(J''_{\rm p})}{kT}\right). \quad (6)$$

We tried to solve the above equation numerically for the $J''_{\rm o} = 1$ and $J''_{\rm p} = 0$ states ($v'' = 0$) to obtain the T_{01} rotational temperature. The observed $N_{\rm ortho}/N_{\rm para} = 0.64 \pm 0.21$ was calculated from the column densities of ortho and para H$_2$ states on the $v'' = 0$ vibrational level (see Table 1). Figure 4 presents the righthand side of Eq. (6) and the ratio of observed column densities (left side of Eq. (6)), together with maximal errors. As we see in Fig. 4 the rotational temperature T_{01} can take any value between 0 and 400 K.

Equation (6) can be written in another way by making two assumptions that are not valid in the interstellar medium:

1. $T > 240$ K $\Rightarrow Z_{\rm p}(T)/Z_{\rm o}(T) \approx 1/3$;
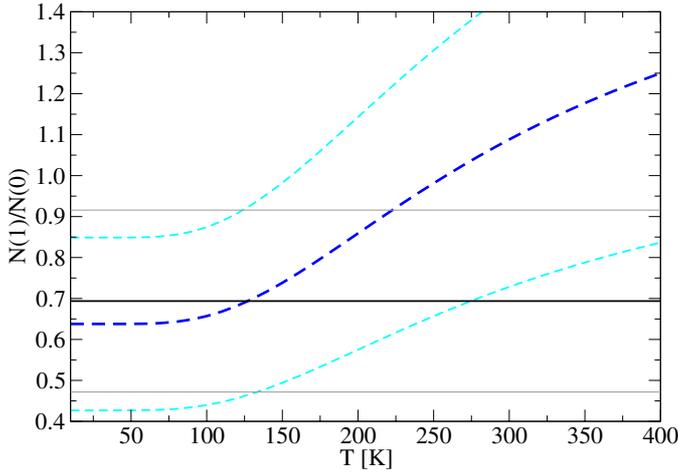2. $N_{\rm ortho}/N_{\rm para} = 3$ as in standard laboratory conditions.

Fig. 4. Theoretical $N(J = 1)/N(J = 0)$ ratio on the $v'' = 0$ vibrational level from Eq. (6) shown as a dark blue dashed line. The light blue dashed lines represent errors introduced by the uncertainty of the N_{ortho}/N_{para} H$_2$ ratio 0.64 ± 0.21. The observed $N(1)/N(0)$ ratio is plotted as a straight black line. The $N(1)/N(0)$ uncertainties are shown as straight gray lines.

Under this assumptions, Eq. (6) for rotational temperature reduces to

$$\frac{N_o(J''_o)}{N_p(J''_p)} = \frac{g_I(1)g_J(J''_o)}{g_I(0)g_J(J''_p)} \exp\left(-\frac{E(J''_o) - E(J''_p)}{kT}\right), \quad (7)$$

and T_{01} is the same as the temperature T_{OP} of ortho-para thermal equilibrium.

The rotational temperatures T_{02} and T_{13} involve rotational levels of the same spin isomers of H$_2$, and do not depend on the total N_{ortho}/N_{para} H$_2$ ratio and on the partition function. For the cloud towards HD 37903, the $T_{02} = 132 \pm 14$ K and $T_{13} = 172 \pm 9$ K. However, the T_{12} temperature (which involves both ortho and para spin isomers) calculated from Eq. (6) is 133^{+37}_{-25} K, while using Eq. (7) gives an incorrect temperature of 263 ± 89 K.

A good illustration that Eq. (6) must be used can be the $v'' = 1$ level. On the $v'' = 1$ level, the temperature $T_{12} = 1223$ K (levels ortho and para) is close to the $T_{02} = 921$ K and $T_{13} = 1090$ K temperatures calculated from the same spin isomers. The temperature calculated with the traditionally used Eq. (7) is negative $T = -466$ K!

The O/P H$_2$ ratio $(O/P)_{v''=1-14} = 1.35 \pm 0.18$ was calculated by summing ortho and para H$_2$ on vibrational levels $v'' = 1-14$. It is a bit lower than O/P $= 1.45 \pm 0.08$, as given by Meyer et al. (2001). We also used the method proposed by Wilgenbus et al. (2000) to calculate O/P H$_2$ from individual ortho levels, specially $J''_o = 1$ and 3 on $v'' = 0$. For the $v'' = 0$ $J'' = 1$ ortho state, the O/P differs significantly from the $(O/P)_{v''=1-14} = 1.35$ value and is equal to $(O/P)_{J''=1} = 0.63 \pm 0.11$. Also for the $v'' = 0$ $J'' = 3$ ortho state, the observed O/P is low, only $(O/P)_{J''=3} = 0.70 \pm 0.07$. For higher rotational and vibrational levels, the Wilgenbus et al. (2000) method gives $(O/P)_{J_o}$ close to 1.3 derived for excited vibrational H$_2$ states.

The rotational temperatures for vibrational levels $v'' = 1-14$ for para H$_2$ were obtained from the linearized Boltzmann distribution:

$$\ln \frac{N_p(J''_p)}{g_I(0)g_J(J''_p)} = \ln N_p(0) - \frac{E(J''_p)}{kT_v}. \quad (8)$$

An analogous equation was used for distribution of the ortho H$_2$ states. Figure 3 shows the lefthand side of Eq. (8) versus E/k.
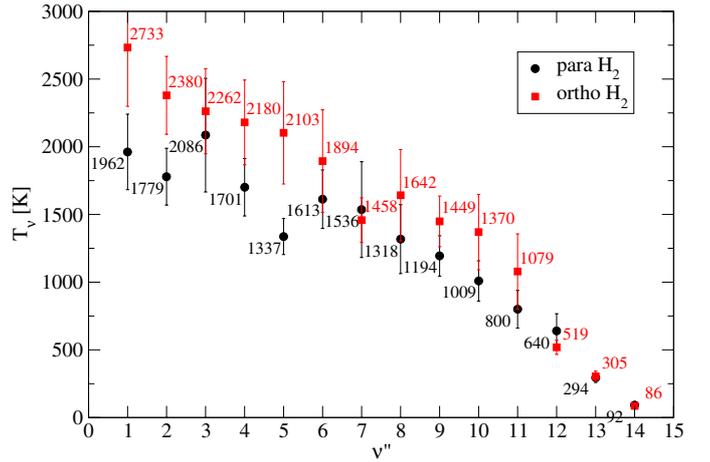
Fig. 5. Rotational temperatures for para and ortho H$_2$ toward HD 37903 as a function of the vibrational number v''.

Table 2. Rotational temperatures for para and ortho H$_2$ as a function of the vibrational level v''.

v''	T_{para} [K]		T_{ortho} [K]	
1	1962	±279	2733	±434
2	1779	±210	2380	±288
3	2086	±420	2262	±314
4	1701	±212	2180	±313
5	1337	±133	2103	±378
6	1613	±216	1894	±379
7	1536	±354	1458	±165
8	1318	±255	1642	±338
9	1194	±149	1449	±187
10	1009	±149	1370	±278
11	800	±139	1079	±278
12	640	±127	519	±53
13	294	±35	305	±38
14	92	±3	86	±9

Levels fulfilling the Boltzmann distribution should be placed on a straight line on this plot. On the $v'' = 0$ vibrational level, which is partially populated by collisions, the occupation of rotational levels does not follow a straight line, therefore the rotational temperature was not calculated for the $v'' = 0$ vibrational level. For both spin isomers and for vibrational levels $v'' = 1-14$ the temperature was calculated using the the linear regression method. The inverse of the line inclination $(-1/T_v$ in Eq. (8)) gives us the rotational temperature. The resulting temperatures are presented in Table 2 and in Fig. 5. The rotational temperatures for the ortho isomer are usually higher than for the para H$_2$. However, the ortho H$_2$ rotational temperatures calculated from levels $J_o = 1$ to penultimate J_o ortho state are in conformity with the para H$_2$ rotational temperatures, so the assumption that the rotational temperatures T_v are the same for ortho and para H$_2$ seems justified. The rotational temperatures fall linearly with the increasing vibrational level.

4. Model

We used the Meudon PDR code (Le Petit et al. 2006) to calculate a model of the interstellar medium in the direction of HD 37903. The interstellar reddening $E(B-V) = 0^m35$ and $R_V = 5.5$ was chosen to match the values used by Meyer et al. (2001). The radiation source is the HD 37903 star (B 1.5 V spectral type). The model includes 300 H$_2$ ro-vibrational levels and uses exact

Table 3. Comparison of cloud models toward HD 37903.

	This paper	Meyer et al. (2001)	Lee et al. (2002)
telescope	HST STIS and FUSE	HST STIS	BEFS ORFEUS
H$_2$ levels	$v'' = 0$–14 $J'' = 0$–13	$v'' = 1$–14 $J'' = 0$–13	$v'' = 0$ $J'' = 0$–5
R_V	5.5	5.5	4.1
n_H [cm^{-3}]	544–1874	130–8800	5600
d [pc]	0.45	0.5	0.2
T_{kin} [K]	110–377	400	—

computation of radiative transfer in H$_2$ spectral lines. The cosmic rays ionization flux was set to 5×10^{-17} s^{-1}. The model is isobaric with thermal balance.

Our models were all two-sided models with an interstellar radiation field on the observer's side equal to one "Draine" unit. The interstellar radiation field on the star side was varied from 1 to 10^4 "Draine" units. The best model was chosen among 6917 different models by minimizing the sum

$$\sum_{v'',J''} w_{v'',J''} \left(\log \frac{N_{obs}(v'',J'')}{N_{obs}(0,0)} - \log \frac{N_{model}(v'',J'')}{N_{model}(0,0)} \right)^2 , \quad (9)$$

where the weights $w_{v'',J''}$ were chosen such, that the levels populated mainly by collisions $J'' = 0$–6 ($v'' = 0$) have the same influence on the final sum as the rest of the levels ($v'' > 0$ and $v'' = 0$ $J'' = 7$–13), which are populated by fluorescence.

We varied the star–cloud distance, hydrogen density, and the interstellar radiation field on the star side in order to find a model that matches the observations. Table 3 compares our best model and models presented by Meyer et al. (2001) and Lee et al. (2002). The star-cloud distance of 0.45 pc, which is responsible for filling the fluorescence H$_2$ levels, is similar in our model and in the model presented by Meyer et al. (2001) ($d = 0.5$ pc). Our cloud kinetic temperature (connected with the collisional-filled levels) equals $T_{kin} = 377$ K on the star side of the cloud and $T_{kin} = 110$ K on the observer's side. The hydrogen density obtained in our best model changes from $n_H = 544$ cm^{-3} on the star side to 1874 cm^{-3} on the observer's side. The interstellar radiation field on both sides of our best cloud model is one "Draine" unit. The hydrogen density and gas kinetic temperature in the PDR model of interstellar cloud toward HD 37903 is shown in Fig. 6.

The O/P on excited ($v \geq 1$) vibrational states is equal to 1.57 in our model. The kinetic temperature in our model is higher than the T_{OP} derived from the $v = 0$, $J = 0$ and 1 levels. However, the bulk of molecular hydrogen may be placed in different part of the cloud than H$_2$ in excited states. This behavior is described by Boissé et al. (2005) for the cloud toward HD 34078.

5. Conclusions

The molecular cloud toward HD 37903 presents a rare type of spectrum with a large number of absorption lines arising from H$_2$ on vibrationally excited states. We determined the column densities of 191 H$_2$ ro-vibrational energy levels using the HST and FUSE ultraviolet spectra.
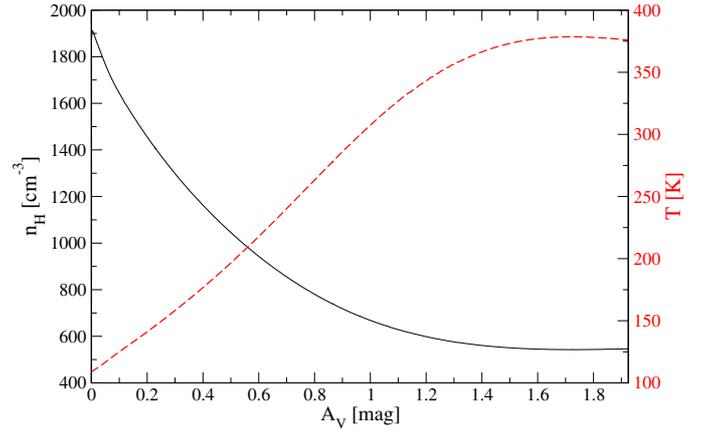

Fig. 6. The hydrogen density (black line) and gas kinetic temperature (dashed red line) in the PDR model of interstellar cloud toward HD 37903.

Column density of molecular hydrogen toward HD 37903 on all observed H$_2$ levels is $N(H_2) = 9.6 \times 10^{20}$ cm^{-2}, the hydrogen molecular fraction equals $f(H_2) = 0.56$, and the rotational temperatures are $T_{02} = 132$ K and $T_{13} = 172$ K. Our principal results follow

- The temperature calculated from the two lowest rotational levels ($J'' = 0, 1$) is a temperature of thermal equilibrium between the ortho and para spin isomers and is equal to 67 K.
- The formula for rotational temperatures calculated across the ortho-para divide (like T_{12}) should include the $(O/P)_v$ H$_2$ ratio.
- The ortho to para H$_2$ ratio is different on the ground vibrational level and in excited states. The O/P H$_2$ ratio equals 1.35 for the excited levels, but for the $J'' = 1$ ortho state ($v'' = 0$) the O/P is only $(O/P)_{J''=1} = 0.63$.
- The best PDR model for the cloud toward HD 37903 gives a gas kinetic temperature $T_{kin} = 110$–377 K, hydrogen density $n_H = 544$–1874 cm^{-3}, and star-cloud distance of 0.45 pc.

References

Abgrall, H., Roueff, E., Launay, F., & Roncin, J.-Y. 1994, Can. J. Phys., 72, 856
Abgrall, H., Roueff, E., & Drira, I. 2000, A&AS, 141, 297
Black, J. H., & Dalgarno, A. 1976, ApJ, 203, 132
Boissé, P., Le Petit, F., Rollinde, E., et al. 2005, A&A, 429, 509
Diplas, A., & Savage, B. D. 1994, ApJS, 93, 211
Draine, B. T., & Bertoldi, F. 1996, ApJ, 468, 269
Federman, S. R., Cardell, J. A., van Dishoeck, E. F., Lambert, D. L., & Black, J. H. 1995, ApJ, 445, 325
Jensen, A., Snow, T., Sonneborn, G., & Rachford, B. 2010, ApJ, 711, 1236
Le Bourlot, J. 2000, A&A, 360, 656
Le Petit, F., Nehmé, C., Le Bourlot, J., & Roueff, E. 2006, ApJS, 164, 506
Lee, D.-H., Min, K.-W., Federman, S. R., et al. 2002, ApJ, 575, 234
Meyer, D. M., Lauroesch, J. T., Sofia, U. J., Draine, B. T., & Bertoldi, F. 2001, ApJ, 553, L59
Rachford, B. L., Snow, T. P., Destree, J. D., et al. 2009, ApJS, 180, 125
Wilgenbus, D., Cabrit, S., Pineau des Forêts, G., & Flower, D. R. 2000, A&A, 356, 1010